AIMS Environmental Science

AIMS Environmental Science, 4(6): 788-808.
DOI: 10.3934/environsci.2017.6.788
Received: 01 August 2017,
Accepted: 15 December 2017,
Published: 25 December 2017

http://www.aimspress.com/journal/environmental

Research article

Variability in the organic ligands released by *Emiliania huxleyi* under simulated ocean acidification conditions

Guillermo Samperio-Ramos[1], J. Magdalena Santana-Casiano[1,*], Melchor González-Dávila[1], Sonia Ferreira[2] and Manuel A. Coimbra[2]

[1] Institute of Oceanography and Global change, University of Las Palmas de Gran Canaria, Tafira Campus, 35017 Las Palmas, Spain
[2] QOPNA, Department of Chemistry, University of Aveiro, Portugal

*** Correspondence:** Email: magdalena.santana@ulpgc.es; Tel: +34928454448; Fax: +34928452922.

Abstract: The variability in the extracellular release of organic ligands by *Emiliania huxleyi* under four different pCO_2 scenarios (225, 350, 600 and 900 μatm), was determined. Growth in the batch cultures was promoted by enriching them only with major nutrients and low iron concentrations. No chelating agents were added to control metal speciation. During the initial (IP), exponential (EP) and steady (SP) phases, extracellular release rates, normalized per cell and day, of dissolved organic carbon (DOC_{ER}), phenolic compounds (PhC_{ER}), dissolved combined carbohydrates ($DCCHO_{ER}$) and dissolved uronic acids (DUA_{ER}) in the exudates were determined.

The growth rate decreased in the highest CO_2 treatment during the IP (<48 h), but later increased when the exposure was longer (more than 6 days). DOC_{ER} did not increase significantly with high pCO_2. Although no relationship was observed between $DCCHO_{ER}$ and the CO_2 conditions, DCCHO was a substantial fraction of the freshly released organic material, accounting for 18% to 37%, in EP, and 14% to 23%, in SP, of the DOC produced. Growth of *E. huxleyi* induced a strong response in the PhC_{ER} and DUA_{ER}. While in EP, PhC_{ER} were no detected, the DUA_{ER} remained almost constant for all CO_2 treatments. Increases in the extracellular release of these organic ligands during SP were most pronounced under high pCO_2 conditions. Our results imply that, during the final growth stage of *E. huxleyi*, elevated CO_2 conditions will increase its excretion of acid polysaccharides and phenolic compounds, which may affect the biogeochemical behavior of metals in seawater.

Keywords: *Emiliania huxleyi*; acidification; extracellular release; phenolic compounds dissolved uronic acids

1. Introduction

Increasing atmospheric carbon dioxide levels causes rapid alterations of the physical and chemical seawater conditions, affecting ecosystem dynamics [1]. About 30% of the CO_2 emitted to the atmosphere by human activities since preindustrial times has been tempered by oceanic uptake, causing wholesale shifts in seawater carbonate chemistry [2]. Moreover, emission projections of CO_2 for this century expect an important increase in total dissolved inorganic carbon and a concomitant decrease in pH, from its current value of 8.1 to 7.8 [3]. This last process, termed ocean acidification, may increase carbon fixation rates in some photosynthetic organisms [4]. Therefore, primary producers, which modify the concentration of CO_2 in the surface natural water, play an important role in the global biogeochemical carbon cycle, affecting the net CO_2 flux across the air-sea interface [5].

The extracellular release of dissolved organic carbon, normalized by cell (DOC_{ER}), is an excretion rate, which indicates the discharge to the medium of recently fixed inorganic carbon. In highly productive marine systems, the release of dissolved organic compounds by phytoplankton can significantly contribute to total primary production [6]. Accordingly, autotrophic DOC_{ER} plays a key role in the biogeochemical balance of ocean carbon, contributing decisively to the biologically-mediated carbon cycle [7,8]. In the open ocean, it represents the main input of reactive organic carbon in the photic layer [9], followed by cell lysis [10], heterotrophic organic exudation, and grazing [11]. Nevertheless, the variations projected for the marine carbonate chemistry [3] might decrease the need for employing CO_2-concentrating mechanisms in autotrophic microorganisms [12], modifying the carbon fixation efficiency and, consequently, the release of organic matter by marine phytoplankton [13].

Although only a small fraction of marine autotrophic DOC has been identified [14], when biological production and DOC-loss processes are decoupled, either temporarily or spatially, combined carbohydrates (CCHO) and phenolic compounds represent an important fraction of reactive dissolved organic matter in seawater [15,16]. In the last years, several studies of the distribution of different biochemical components in the ocean have been carried out, both in their dissolved and/or particulate phases, with CCHO shown to be the dominant constituent in the colloidal size fraction [17]. Dissolved combined carbohydrates (DCCHO) are the major component of reactive organic carbon and can account for up to 10% of DOC in open ocean [18], whereas in continental margin and coastal systems they represent between 15% and 35% of DOC [19,20]. Autotrophic DCCHO are a robust indicator of the diagenetic state of organic matter, since most of the DCCHO produced by phytoplankton are a carbon active reservoir for bacterioplankton [21], especially in an ocean acidification context [22,23]. Extracellular polymeric substances released by microorganisms during their growth contain a high proportion of dissolved uronic acids (DUA) [24,25], a class of sugar acids with carboxylic acid functional groups, which confer a net negative charge, forming resilient linkages between the polymer chains [26]. Coagulation of those aggregates involves the formation of transparent exopolymeric particles, which play an important role in the sink of marine DOC [27,28].

Phenolic compounds (PhC) are also naturally present in marine systems, since they are considered to be one of the principal functional groups in humic substances [29]. Phenols can also be released from polymers, during both photochemical decomposition and biodegradation of natural organic matter [30,31]. Therefore, river discharge and the subsequent physical mixing processes of seawater play an important role in controlling the concentration and distribution of PhC in the ocean [31]. Phenolic fractions contribute significantly to the fluorescence of organic matter extracted from interstitial water of

marine sediments [32] and comprise an important part of the DOC pool, accounting to up to 5% of that, accrued in the surface waters of subtropical ocean gyres [33]. Moreover, PhC are excreted by a wide range of marine macroalgae as secondary metabolites [34]. Although the regulatory processes of exudation of phenolic compounds by phytoplankton have not been clearly established, recently an increase in the phenolic content of exudates in diatoms (*Phaeodactylum tricornutum*) and green algae (*Dunaliella tertiolecta*), were measured when those microorganisms grew under iron deficient scenarios [35,36], suggesting that phenolic release might be a response to unfavorable growth in iron limited conditions.

Phenolic compounds and dissolved uronic acids can form complexes with iron through hydroxyl and carboxylic acid groups [37,38]. Both catechol, a frequent and reactive dihydroxyphenolic moiety found in exudates of phytoplankton [39], and carboxylic acids bind iron to produce relatively stable Fe-organic complexes, preventing iron precipitation [40,41] and increasing the iron bioavailability in seawater [42,43]. This is particularly important in a significant proportion of the open ocean, where iron limits phytoplankton growth [44]. Therefore, in some Fe-limited regions, phytoplankton could be a significant source of PhC and DUA [45,46]. Nevertheless, the fractional contribution of phenolic PhC and DUA to the pool of autotrophic DOC production is controlled by the physico-chemical parameters of the extracellular medium, such as temperature, pH, light, and bioavailability of inorganic nutrients [4,36,47,48]. Ocean acidification alters the physiologic pathways of the coccolithophorid *Emiliania.huxleyi*, such as the Krebs cycle and mitochondrial respiration, due to an increase in the production of PhC [49]. Such elevated CO_2 conditions can also stimulate the release of DUA in eukariota community [50]. In fact, chemostat experiments have exhibited an increase in the production of saccharides in *E.huxleyi*, as well as magnification in the transfer of dissolved high molecular weight carbohydrates to transparent exopolimeric particles, by abiotic aggregation processes [51]. Nevertheless, an experimental assessment of releasing *E.huxleyi*-derived Fe-ligands under ocean acidification conditions has not been conducted without continued nutrient supply, which regulates the rate of growth and, therefore, the physiological status of microorganisms. Moreover, the chemical variation of Fe-binding agents due to ocean acidification, along the coccolithophorid growth curve remains unclear, given that growth phases have been shown to affect the composition of DOC released by phytoplankton [52].

In order to improve our understanding of the extracellular release of organic ligands excreted by phytoplankton under future and pre-industrial marine carbon chemistry conditions, we have conducted several microcosm experiments with *E. huxleyi* where the dissolved inorganic carbon and the pH have been manipulated. The coccolithophorids play a key role in the biogeochemical cycle of carbon and are particularly sensitive to ocean acidification, due to the production of calcite coccoliths [53]. The high genomic plasticity of coccolithophorid *E.huxleyi* causes it to thrive in large-scale episodic blooms in a wide variety of habitats [54]. Therefore, the objectives of this research are (1) to study the variation, normalized per cell and day, of DOC, saccharides (i.e., DCCHO and DUA) and phenolic compounds in the exudates of *E. huxleyi* during the different growth stages, (2) to quantify the contribution of organic compounds excreted to DOC, and (3) to carry out a statistical analysis for growth rates and the release rates of DOC and organic ligands, taking into account the effect of CO_2 conditions on the *E. huxleyi* batch cultures under low iron state.

2. Materials and methods

2.1. Set-up

The carbonate chemistry in the culture medium was manipulated through a system (Figure 1) based on bubbling a gas mixture of CO_2-free air and pure CO_2 [55]. To ensure quasi-constant seawater carbonate chemistry (Table 1), when the seawater pH values reached the target value, a solenoid valve, connected both to gas cylinders and a pH controller, modulated the CO_2 flux, maintaining the set pH (±0.02). pH was measured on the free hydrogen ion scale, $pH_F = -\log [H^+]$ with a Ross Combination glass body electrode calibrated daily with TRIS buffer solutions. To establish the present and future CO_2 ocean conditions, four experimental scenarios, based on projections by the Intergovernmental Panel on Climate Change [3] were fixed: preindustrial, close to contemporary and two futures ocean acidification conditions with pCO_2 225, 350, 600 and 900 µatm, respectively. Consequently, the aeration with a CO_2-air-mixture generated constant pH values of 8.25, 8.10, 7.90 and 7.75 (Table 1). Microcosms were carried out in autoclaved and closed 2.5 L polycarbonate cylindrical tanks to avoid gas exchange between the medium and the ambient atmosphere and to prevent variation in salinity by evaporation. To ensure gas homogeneity in the solution and to keep cells in suspension, the cultures were mixed at 60 rpm with a teflon-coated magnetic stirrer. Material, including cell incubators, gas inoculators and tubes connected to them, were cleaned according to a standard protocol [56] and subsequently sterilized by autoclaving at 121 ºC for 30 min before usage.

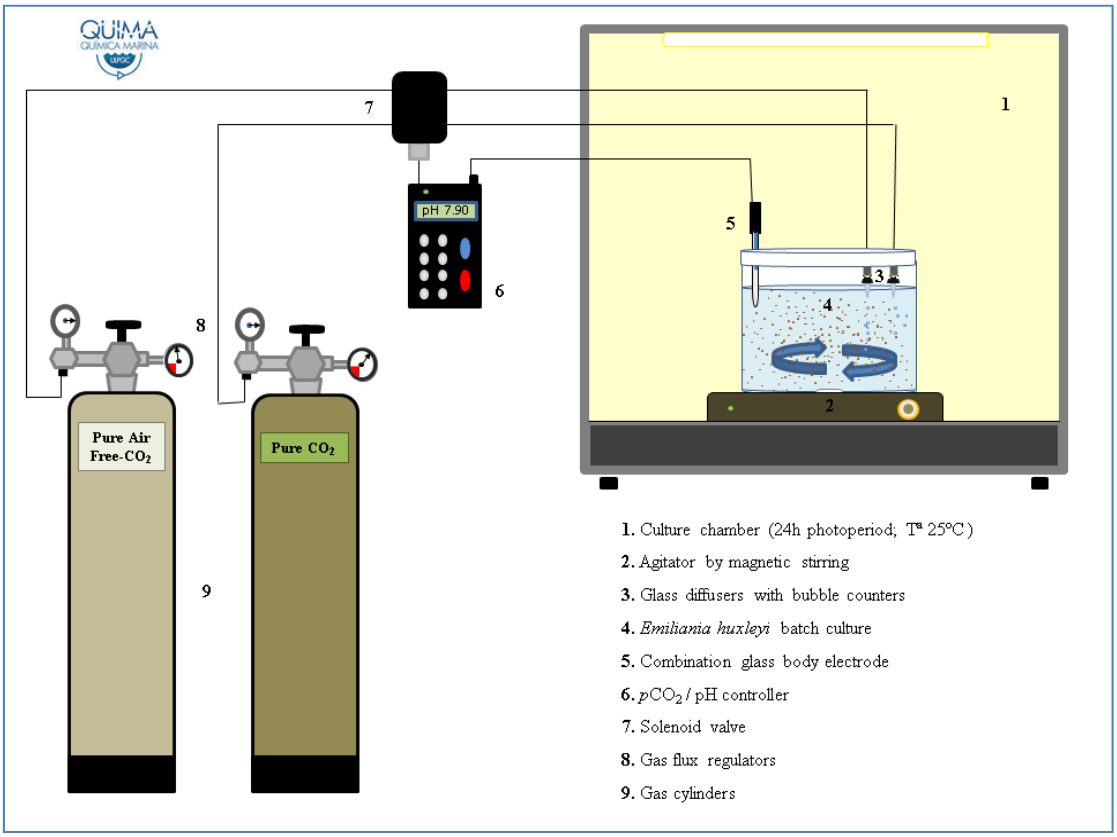

Figure 1. CO_2/pH perturbation experiment set-up, indicating the components.

Table 1. Carbonate chemistry parameters, for each CO_2 treatment: pH (total scale), total alkalinity (TA) normalized to S‰ = 35, total dissolved inorganic carbon concentration ([DIC]) and calculated pCO_2 (µatm) Temperature 25 ºC. Mean values and standard errors (in parentheses) were derived from sampling (n = 6).

pCO_2 treatment (µatm)	pH_T (±0.02)	TA (µmol kg^{-1})	[DIC] (µmol kg^{-1})	pCO_2 (µatm)
225	8.25	2355.5 (±11.7)	1886.8 (±19.0)	223.2 (±1.2)
350	8.10	2353.7 (±14.0)	1991.6 (±16.2)	351.4 (±3.9)
600	7.90	2368.3 (±14.8)	2106.6 (±18.1)	607.7 (±5.3)
900	7.75	2383.6 (±10.9)	2196.3 (±12.8)	917.8 (±12.6)

2.2. Cultures

The axenic culture stock of E. *huxleyi* was supplied by the Spanish Bank of Algae (BEA, Taliarte). The stock and experimental cultures were placed in an incubator clean chamber (Friocell FC111) at a constant temperature of 25 ºC, under complete photoperiod (24 h) with light intensity of 200 µmol photons m^{-2}. In order to pre-adapt to each CO_2 treatment, the stock cultures were maintained under the experimental conditions for 48 h before starting each experiment, allowing the acclimatization to CO_2 perturbation, in order to avoid short-term stress effects on coccolithophorid physiology. Experimental cultures were grown in sterile filtered (0.1 µm) North Atlantic seawater (S = 36.48) obtained at the ESTOC site (29º10' N, 15º30' W). When the seawater reached the desired value of pCO_2/pH, the coccolithophorids were inoculated in the batch cultures to a density of 10^6 cells L^{-1}. Stock and experimental cultures were monitored for contamination and cell densities using a microscope and a hematocytometer (Microbiotest, Inc.). Immediately and in order to promote a useful development during the coccolithophorid growth, nitrate and phosphate were added at a ratio of 30:1 [28], yielding initial concentrations of ortophosphate (PO_4^{3-}) and nitrate (NO_3^-) of 28 and 850 µM, respectively. To promote coccolithophorid growth, iron was added to seawater from a stock solution (1 mM) of ferric chloride (Sigma), making an initial concentration of 2.5 nM. All nutrients used in the batch cultures were trace analytical grade. To carry out the organic assays, the seawater enriched with exudates was sampled and filtered using acid cleaned and combusted polycarbonate (Nucleopore) syringe-filters (0.45 µm), to avoid cell breakage.

2.3. Total Alkalinity and total dissolved inorganic carbon

Samples for total alkalinity were potentiometrically titrated with HCl to carbonic acid end point using the VINDTA 3C system as described in detail by González-Dávila and co-workers [57]. The titration of the different CRMs (provided by A. Dickson at Scripps Institution of Oceanography) was used to test the performance of the titration system giving values with an accuracy of ±1.5 µmol kg^{-1} and a standard deviation of 6 µmol kg^{-1}. The precision (between-bottle reproducibility) as judged from regular measurements of duplicate samples was 0.5 µmol kg^{-1}. Dissolved inorganic carbon was analyzed with coulometer determination. The accuracy and standard deviation obtained after CRMs titration were ±1.0 and 11.8 µmol kg^{-1} respectively. In order to compare with other seawater values,

dissolved inorganic carbon and total alkalinity (X) were normalized (X_n) to a constant salinity ($S_{ref} = 35$), $X_n = (X/S_{sample})\cdot S_{ref}$. The package Seawater Carbonate (Seacarb version 3.0), developed with R (R development Core Team) was used to calculate the values of pCO_2, using the experimental results of pH, dissolved inorganic carbon and total alkalinity and considering the carbonic acid dissociation constants of Millero and coworkers [58].

2.4. Dissolved organic carbon (DOC)

DOC concentration in samples (both in seawater and in the seawater enriched with *E .huxleyi* natural exudates) was monitored using a Total Organic Carbon analyzer (Shimadzu TOC-V) previously calibrated from standard curves (20 to 300 μmol C L^{-1}) with a potassium hydrogen phthalate standard (Sigma-Aldrich) [59]. DOC reference material (Dr. Hansell; University of Miami) was analyzed to check for the accuracy and precision of the instrument. The method had an uncertainty of 3% and a detection limit of 1.3 μmol C L^{-1}. The measures of certified reference material had a standard deviation of 0.99 μmol C L^{-1}. The instrument blank (3–10 μmol C L^{-1}) was measured using UV-irradiated Milli-Q water and was subtracted from each sample.

2.5. Phenolic compounds (PhC)

The Arnow test [60] enabled the selective detection of hydroxyphenolic compounds in seawater enriched with exudates of *E. huxleyi* (5 mL, filtered by 0.45 μm) by addition of hydrochloric acid (5 mL; 0.5 M), followed by addition of 5 mL (0.5 M) of sodium molybdate (Sigma-Aldrich) and 5 mL (0.5 M) of sodium nitrite (PanReac). Then, sodium hydroxide (Sigma) was added in excess (5 mL; 1 M). Maximum absorbance was read at 510 nm using a UV-VIS spectrophotometer (S4000, Ocean Optics^{TM}), connected to a 5 m long waveguide capillary flow cell (World precision instruments^{TM}), which allowed to reach a detection limit of 2×10^{-8} M. The standard employed for the assay was catechol (Sigma-Aldrich) and Mili-Q water with the reagents was used as blank.

2.6. Total dissolved combined carbohydrates (DCCHO)

The levels of DCCHO both in seawater and in seawater enriched with exudates of *E.huxleyi* were analysed by the method developed by Myklestad and co-workers [61] with slight amendments [19], which is based upon oxidizing the free reduced DCCHO with the 2,4,6-Tris(2-pyridyl)-s-triazine (TPTZ; Sigma-Aldrich). The assay involved the acid hydrolysis of the sample (4 mL) with HCl (0.4 mL), in a sealed ampoule, for 2 h at 120 ºC. When the solution was neutralised (0.4 mL of 1 M NaOH), 1 mL of the hydrolysate was added to a 1 mL of a 0.7 mM potassium ferricyanide (Sigma-Aldrich), prepared in 1 L of Milli-Q water containing 20 g Na_2CO_3 and 400 mg NaOH. The well-mixed solution was placed in a boiling water bath for 15 min. Then, 1 mL of solution of ferric chloride solution (2 mM) and 1 mL of TPTZ solution (3 M) were promptly added [61] and thoroughly mixed on a Vortex. After 30 min, the absorbance was measured, using UV-VIS spectrophotometer (S4000, Ocean Optics^{TM}), at 595 nm, (S4000, Ocean Optics^{TM}). The standard employed was glucose (Sigma-Aldrich) and the absorbance of the reagent blank in Milli-Q water was subtracted before reading the absorbance of the monosaccharide of each sample.

2.7. Dissolved uronic acids (DUA)

In order to have a measurable level for DUA, the samples were concentrated by rotary evaporation, under reduced pressure at 40 ºC. Subsequently, the concentration of DUA was measured according to the method reported by Blumenkrantz and Asboe-Hansen [62] and modified in Bastos and coworkers [63]. 3 mL of 75 mM sodium tetraborate in concentrated sulfuric acid was added to 0.5 mL of the concentrated sample and the resulting solution was heated to 100 °C for 10 min in a boiling water bath. After cooling, 100 µL of 0.15% m-hydroxydiphenyl (Sigma-Aldrich) was added, and the absorbance was determined spectrophotometrically at 525 nm. The reagent blank was considered in order to compute the final concentration of the monosaccharide. Galacturonic acid (Sigma-Aldrich) was used as the standard.

Table 2. Parameters computed during pCO_2/pH treatments for each growth stage. The statisticals computing (Analysis of variance, ANOVA), are also included.

Growth Stages	pCO_2 (µatm)	µ (day^{-1})	DOC_{ER} (fmol C $cell^{-1}$ day^{-1})	PhC_{ER} (fmol C $cell^{-1}day^{-1}$)	$DCCHO_{ER}$ (fmol C $cell^{-1}$ day^{-1})	DUA_{ER} (fmol C $cell^{-1}$ day^{-1})
IP (day 2)	225	1.12 ± 0.03	-	-	38.86 ± 5.94	-
	350	1.18 ± 0.06	-	-	34.59 ± 6.92	-
	600	1.15 ± 0.04	-	-	35.39 ± 6.42	-
	900	1.07 ± 0.06	-	-	35.08 ± 4.82	-
EP (day 5)	225	0.59 ± 0.05	177.06 ± 10.95	-	40.38 ± 4.16	2.27 ± 0.42
	350	0.60 ± 0.04	186.84 ± 52.96	-	45.43 ± 7.20	2.36 ± 0.46
	600	0.62 ± 0.02	196.33 ± 44.01	-	41.14 ± 6.82	2.64 ± 0.90
	900	0.60 ± 0.05	209.74 ± 50.00	-	41.00 ± 3.49	2.35 ± 0.61
SP (day 8)	225	0.13 ± 0.03	333.68 ± 71.35	0.34 ± 0.03	44.43 ± 2.98	5.24 ± 0.41
	350	0.15 ± 0.01	345.75 ± 45.86	0.36 ± 0.02	45.74 ± 4.93	6.25 ± 0.48
	600	0.16 ± 0.02	370.14 ± 15.79	0.40 ± 0.02	47.39 ± 7.36	6.70 ± 0.97
	900	0.19 ± 0.01	384.19 ± 47.40	0.41 ± 0.02	46.95 ± 3.92	7.39 ± 0.30
Factors of variation						
Growth Stages	*F value*	-	25.8422	-	3.4735	80.9422
	p	-	<0.001	-	<0.05	<0.001
Growth Stages x pCO_2	*F value*	-	0.0212	-	0.162	0.9084
	p	-	0.9956	-	0.9855	0.4787
pCO_2 - (IP)	*F value*	1.257	-	-	0.095	-
	p	0.324	-	-	0.962	-
pCO_2 - (EP)	*F value*	0.113	0.3161	-	0.168	0.208
	p	0.949	0.8136	-	0.916	0.888
pCO_2 - (SP)	*F value*	4.228	0.0212	3.765	0.086	6.227
	p	<0.05	0.9956	<0.05	0.967	<0.05

2.8. Data and statistical treatments

The growth rates (μ day^{-1}) were calculated from the changes in the cell number over time and data were fitted to an exponential growth model ($\mu = (\ln N_{t2} - \ln N_{t1})/\Delta t$). The cell densities (N) were determined from the average of 5 experimental batch cultures at each pCO_2 treatment. The goodness of the fit for each curve was estimated by the coefficient of correlation ($r^2 > 0.95$). Under the different CO_2 scenarios, the development of *E. huxleyi* happened according to a sigmoid curve (Figure 2) showing three significantly marked trends in the growth rates, as the culture time elapsed (Table 2). Thus, the measurements of DOC (μmol C L^{-1}), as well as, the determination of organic extracellular release rates (μmol C $cell^{-1}$ day^{-1}), were carried out distinguishing the three stages in the growth curves of *E. huxleyi*: initial (IP, until 2nd day), exponential (EP, from 3rd to 5th day) and steady (SP, from 6th to 8th day) phases (Table 2). The concentrations of, DOC, PhC, DCCHO and DUA were corrected to levels of seawater and the unit utilized was obtained by multiplying the concentration values (μmol L^{-1}) by the number of carbon per mole of compounds used as standards during calibrations (i.e., phthalate, catechol, glucose and galacturonic acid, respectively). Given that the exudation rate of freshly dissolved material is a parameter best specified when it is normalized per cell and day, we followed the procedure in Borchard and Engel [64]. Thus, extracellular release rates (μmol C $cell^{-1}$ day^{-1}) were derived from DOC accumulation rates (μmol C L^{-1} day^{-1}) and variation of the cell densities.

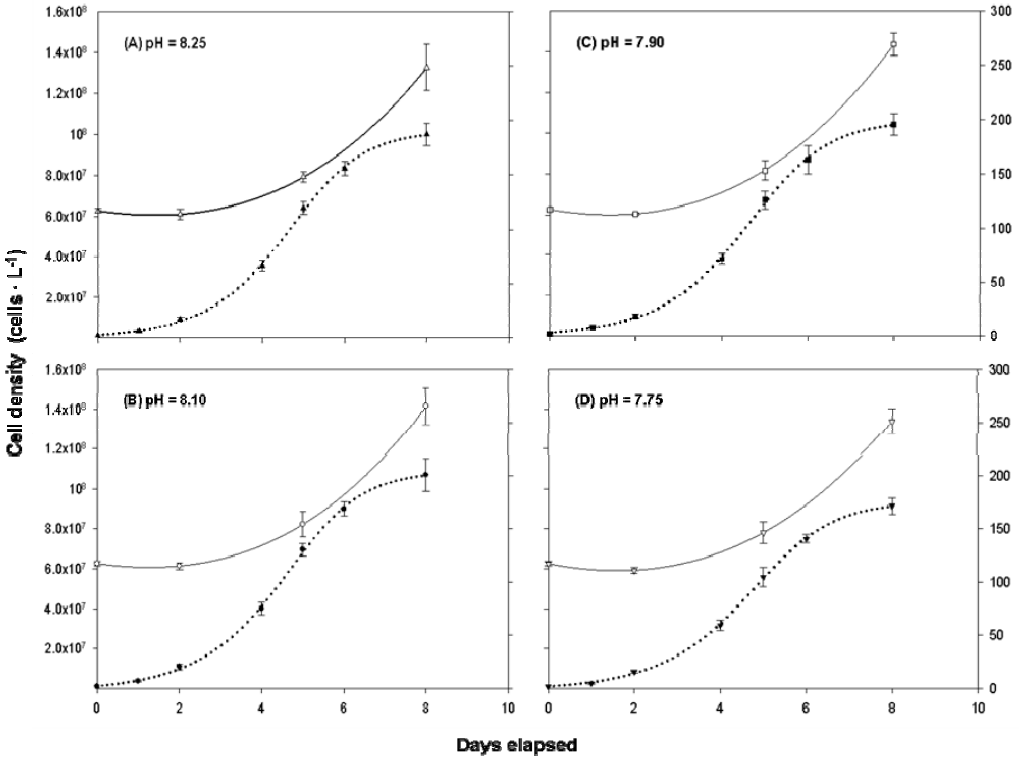

Figure 2. Changes in *Emiliania huxleyi* abundances (broken lines) and dissolved organic carbon (DOC) concentration (solid lines), under different CO_2 conditions, during experimental cultures. Error bars represent ±SE of the mean (n = 5).

R (R Development Core Team, 2008) was used for statistical computing. Analysis of variance (ANOVA) was carried out to test for significant effects of both different pCO_2 treatments and growth stages on the normalized production of DOC, DCCHO and organic ligands (i.e., PhC and DUA) present in the *E.huxleyi* natural exudates during the culture development. A post-hoc test, Tukey's HSD, was used to do a multiple comparison procedure to find means that were significantly different. The assumptions of normality and homoscedasticity were verified using the Shapiro-Wilk and Barlett tests respectively. Regression models were used to assess the relationships between organic parameters. For all statistical procedures, a probability level of $\alpha = 0.05$ was considered.

3. Results and discussion

3.1. Growth rates

Initially, average *E. huxleyi* cell numbers were 10^6 and increased continuously during the 8 days of study to $9.98 \pm 0.53 \times 10^7$ (pCO_2 225 µatm), $1.07 \pm 0.13 \times 10^8$ (pCO_2 350 µatm), $1.04 \pm 0.07 \times 10^8$ (pCO_2 600 µatm) and $9.15 \pm 0.41 \times 10^7$ (pCO_2 900 µatm) (Figure 2). Therefore, acidification conditions did not significantly affect the final cells densities (one-way ANOVA, F-value: 1.327, $p = 0.332$). Nevertheless, to evaluate in detail the effect of pCO_2/pH on coccolithophorids cellular division rates, we distinguished three growth stages separately: the initial phase (IP), the exponential phase (EP) and the steady phase (SP). During the IP, the growth rate showed the lowest values when the microalgae were exposed to the highest CO_2 levels ($\mu = 1.07 \pm 0.05$ day^{-1}), while the maximum growth rates were achieved with pCO_2 350 µatm and 600 µatm ($\mu = 1.19 \pm 0.07$ and 1.15 ± 0.03 day^{-1}, respectively). In EP, the growth rates remained fairly constant under the different CO_2 conditions and were matched to the results found for *E. huxleyi* [65] and other coccolithophorid species [66] in studies conducted in batch cultures. However, during SP, a statistically significant growth rate rise was observed (F-value: 4.228, $p < 0.05$), in response to increasing CO_2 concentration, reaching 0.19 ($\pm$ 0.01) day^{-1} at pCO_2 900 µatm, (Table 2). Our results indicated that the *E. huxleyi* populations adapted to experimental acidification, displaying a slight increase in growth rates during SP. Nevertheless, the highest peaks of algae biomass, 1.07 ($\pm$ 0.10) and 1.04 ($\pm$ 0.06) $\times 10^8$ cells L^{-1}, were recorded in the microcosms with intermediate CO_2 levels (350 and 600 µatm respectively). Over the last decade, studies involving acidification perturbation experiments, carried out with coccolithophorids in batch cultures, have exhibited variability on the specific growth response [67-69], related to intrinsic physiological parameters such as the process of calcification or cell size of the different strains [70]. Environmental conditions such as light intensity [71], temperature [72] or major nutrients availability [73] were also pointed out as decisive co-factors to induce changes in the division rates during CO_2/pH perturbation experiments. However, in the present study, the cultures were kept under identical temperature and photon flux density. In the short term incubations discussed here, we exclude the limitation of P and N as a cause of the decline in growth rates, since both the initial nitrate and phosphate concentrations (850 µM and 28 µM, respectively) are fairly above the half-saturation constant of N and P uptake [74]. *E. huxleyi* has typically been assumed to be a strong competitor under iron deficient conditions [75], even though incubation experiments have provided evidence that iron can limit *E. huxleyi* growth [76]. Although in the open ocean dissolved iron is found at subnanomolar levels [77], the concentrations fixed in the present study (2.5 nM) could be considered as low Fe conditions, since the abundances of *E. huxleyi,*

reached during experimental cultures were between one and three orders of magnitude higher than the biomass of photosynthetic eukaryotes found in different marine systems [78]. Nevertheless, the dissolved iron concentration was not a factor considered during the experiments and therefore the Fe-limitation might not be assured.

3.2. DOC dynamics

From seawater control initial DOC concentrations (117.34 ± 1.97 μmol C L^{-1}) decreased non-significantly during IP (F-value = 2.273, P = 0.156). This decline of DOC levels was slightly affected by CO_2 conditions, since the loss of DOC varied from pCO_2 225 μatm (3.04 ± 2.32 μmol C L^{-1}) to pCO_2 900 μatm (6.19 ± 2.71 μmol C L^{-1}). Pre-sterilization both of seawater and bioreactors allowed to keep a low density of heterotrophic bacteria (<10^6 cell L^{-1}) in the course of the experimental period. Hence, microbial organic matter degradation might explain the decline in DOC levels under the different experimental CO_2 conditions during IP, since in bacterial enzyme's environments, a drop in the pH modifies the ionization state of labile organic matter, exposing the actives sites of their three-dimensional structure [79], and thus accelerating their degradation [23]. DOC sinking might also be due to aggregation of high molecular weight dissolved components, which is increased at high CO_2 levels [80]. We did not measure the transparent exopolymeric particles formation but the aggregation process is highly dependent on the physiological status of the microbial community [81] and its formation occurs after exhaustion of the major nutrients [28]. Therefore, in the short term incubations, conducted under N and P repletion conditions, the relevance of abiotic aggregation processes can be considered negligible.

The incubations showed an increase in the productivity status, achieving autotrophic conditions during the EP and SP (Figure S1, Supporting Information). The accumulation of DOC did not show a significant difference among the CO_2-treatments (F-value = 0.174, P = 0.911 for EP; F-value = 0.474, P = 0.709 for SP). In the same way, Borchard and Engel [51] found no significant effect of pCO_2 on concentrations of DOC during steady state growth in continuous cultures of *E. huxleyi.* Recently, during shipboard bioassay experiments with a natural community from North Sea, neither was not observe any strong or consistent effect of pCO_2 on DOC production [81]. The amount DOC exuded into environment may be highly variable and is a function of the dominant species and its response to changes in the CO_2 conditions [82]. For example, in mesocosms experiments carried out in a high nutrient low chlorophyll region of the Pacific Ocean, pH-dependence of the DOC levels only occurred when diatoms increased their dominance over the haptophyta algae group (i.e., coccolithophorids) [83]. Unlike absolute measures, the organic production rates (i.e., extracellular release) are relatively constant parameters between the different phytoplankton species and only change in response to physiological perturbations produced by environmental factors, such as nutrient availability or CO_2 conditions [51,84].

DOC_{ER} increased as the levels of CO_2 became higher in the culture medium (Figure 3), from 177.06 ± 10.95 fmol C $cell^{-1}$ day^{-1} (pCO_2 225 μatm) to 209.74 ± 50.00 fmol C day^{-1} $cell^{-1}$ (pCO_2 900 μatm) in EP and from 333.68 ± 71.35 fmol C $cell^{-1}$ day^{-1} (pCO_2 225 μatm) to 384.19 ± 47.40 fmol C day^{-1} $cell^{-1}$ (pCO_2 900 μatm) in SP. The increment of pCO_2 in the experimental cultures, from 225 μatm to 900 μatm, enhanced DOC_{ER} by 19% and 15% during EP and SP, respectively. As CO_2 is a key substrate for primary production, the trend of DOC_{ER} with pCO_2 was also in agreement with those obtained during the first week of a long-term mesocosm with a phytoplankton pelagic

community, where the assimilation of inorganic carbon was improved under acidified conditions [85]. Therefore, DOC_{ER} of *E. huxleyi* might have been slightly stimulated by the elevated pCO_2, although the response was highly variable and no significant effect of pCO_2 was determined (Table 1). Our results are also comparable with the range of DOC_{ER} presented by Becker et al. [86] with different strains of cyanobacteria and diatoms. As bioassay time proceeded, from day 5 to 8 (EP to SP), an increase of DOC_{ER} between 83% (pCO_2 225 µatm) and 89% (pCO_2 900 µatm) was estimated. Higher DOC_{ER} in SP compared to the EP have been also noted previously in batch cultures both of diatom [87,88] and coccolithophorids [89,90].

On the other hand, during another Baltic Sea mesoscosm study [91] and also in laboratory incubations [92], the higher CO_2 levels supported the production and release of carbon-rich components by microorganisms. Therefore, in order to ascertain how the CO_2 perturbation experiments, carried out in the present work, condition the composition of organic ligands in natural exudates of *E.huxleyi*, the release of PhC, DCCHO and DUA were monitored.

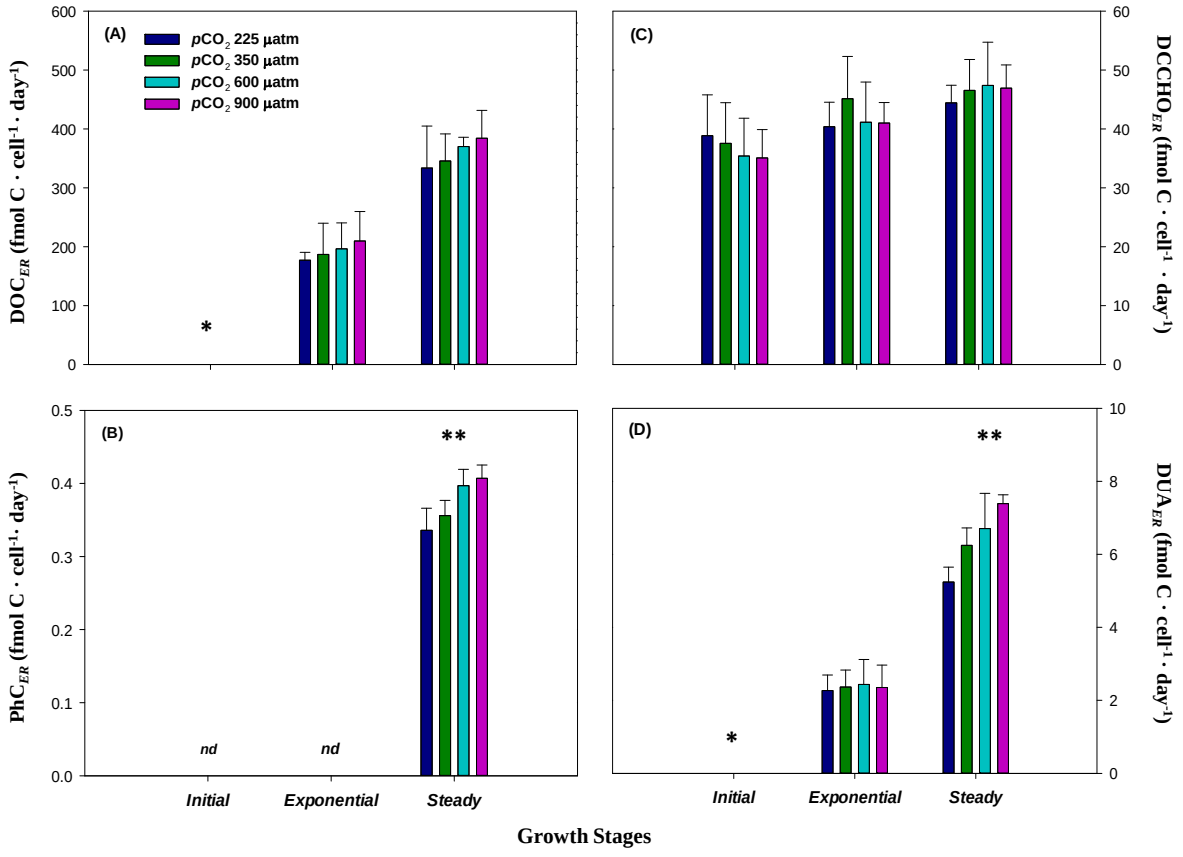

Figure 3. Extracellular release rates (fmol C·cell^{-1} day^{-1}) of (a) dissolved organic carbon (DOC), (b) phenolic compounds (PhC), (c) dissolved combined carbohydrates (DCCHO), and dissolved uronic acids (DUA) for each growth stage, from *Emiliania huxleyi* cultures subject under different CO_2 treatments. Stacked bars show the standard error of replicate samplings (n = 3, 5, 5 and 3 for DOC, Ph, DCCHO and DUA respectively). The following indications: *, *nd* and ** denote: not detected, no significate differences between SW and SW enriched with microalga exudates and statistical differences between pCO_2 treatments respectively.

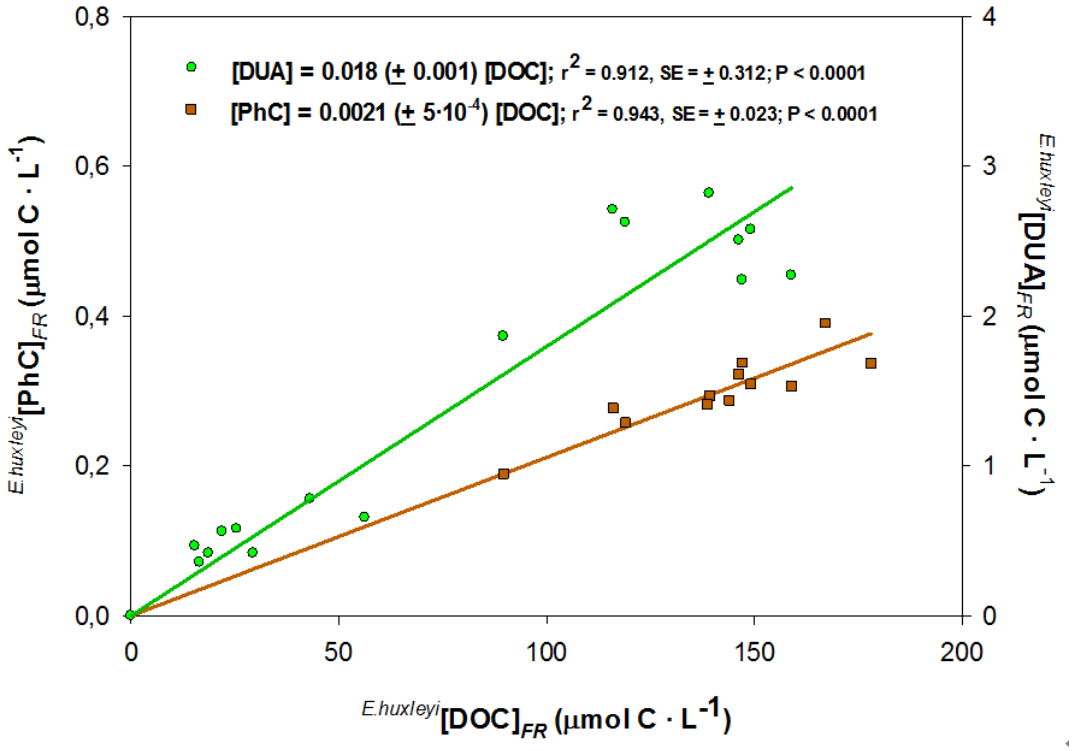

Figure 4. Linear correlations between concentrations of freshly phenolic compounds (PhC) and dissolved uronic acids (DUA) with dissolved organic carbon (DOC), released in *E. huxleyi* cultures.

3.3. Phenolic compounds

Figure 4 shows the strong correlation between the concentrations of freshly produced PhC with DOC, indicating that phenolic compounds made up a relatively constant fraction of the organic material excreted by *E.huxleyi*. However, the dissolved phenolic compounds were only detected in SP and their release rate was affected by CO_2 conditions. Extracellular release of phenolic compounds (PhC_{ER}) was statistically higher (Table 1) at pCO_2 900 µatm (0.41 ± 0.02 fmol C cell^{-1} day^{-1}) than at pCO_2 225 µatm (0.34 ± 0.03 fmol C cell^{-1} day^{-}1; Tukey contrast: t value = 2.898; $p < 0.05$) and 350µatm (0.36 ± 0.02 fmol C cell^{-1}day^{-1}; Tukey contrast: t value = 2.495; $p < 0.1$). The biosynthesis of PhC has implications for grazers, pathogens [93], for preventing photo-damage [94] and free radical scavenging activity [95]. Phytoplankton can also regulate the bioavailability of trace metals through the production and release of phenolic compounds [39]. However, the mechanism by which autotrophic organisms regulate their phenolic exudation in response to increased pCO_2 is also not clear. Jin et al. [49] have reported that the high CO_2-induced changes in seawater carbonate chemistry enhanced the intracellular production of phenolic compounds in *E.huxleyi*. Recently, another study has also determined how a natural acidification event regulates the biosynthesis of phenolic compounds in calcified macroalgae communities, although the magnitude of their response depends on nutrient and light levels [96]. Our data (Figure 3) suggest that ocean acidification might significantly intensify the PhC_{ER}, when *E.huxleyi* grows under low iron conditions. Thereby, an increase in the phenolic fraction in the exudates of *E.huxleyi* might improve its capacity for iron

acquisition [41,42] under an ocean acidification scenario, in which the bioavailability of Fe for eukaryote phytoplankton seems to decline [97]. Similarly, under an iron starvation state, some prokaryote microorganisms exudate ferric chelators (i.e., siderophores) [98] capable of solubilizing, capturing, and delivering iron to the cell through protein-specific transport systems [99]. In addition, marine siderophore production seems to be optima in buffered acidified media [100], although in natural seawater the pH-dependence on siderophore release remains unknown.

3.4. Dissolved combined carbohydrates

The initial concentration of DCCHO in the cultures was 24.14 ± 0.88 μmol C L^{-1}. DCCHO increased in solution during *E.huxleyi* growth, representing a substantial fraction of freshly produced DOC during all growth stages. The levels of freshly produced DCCHO were very close among the different CO_2 treatments (data not shown). Figure S2 (Supporting Information) shows the significant linear relationships between the concentrations of freshly DCCHO and DOC yielded, where the contribution of DCCHO to excreted DOC was higher during EP (18–37%) than during SP (14–23%). Our data are comparable with that obtained by Hung et al. [19] in high productivity Gulf of Mexico waters, where the authors also linked the increase in DCCHO levels to the different peaks of chlorophyll *a* concentration, found in that region.

Extracellular release of dissolved combined carbohydrates ($DCCHO_{ER}$) during the initial-state of *E. huxleyi* growth were 38.9 ± 6.9 fmol C $cell^{-1}$ day^{-1}, 34.6 ± 7.7 fmol C $cell^{-1}$ day^{-1}, 35.4 ± 6.4 fmol C $cell^{-1}$ day^{-1} and 35.1 ± 4.8 fmol C $cell^{-1}$ day^{-1} for pCO_2 225, 350, 600 and 900 μatm respectively (Figure 3), increasing significantly as time elapsed from EP until the cultures reached the SP (Table 2). Extracellular release rates of DOC and DCCHO slightly differ from those determined by Borchard and Engel [51] during steady-state growth under CO_2 simulated condition in phosphorus controlled chemostats. Those differences might be attributed both to different coccolithophorid strains being evaluated and experimental drawing, as well as the physico-chemical parameters fixed during the growth of *E. huxleyi*, such as light:dark cycle, photon intensity, and nutrient status (i.e., P and Fe). In agreement with our results, these previous results did not reflect a relationship among $DCCHO_{ER}$ and CO_2 conditions. For the batch cultures here presented the $DCCHO_{ER}$ was statistically lower in IP than EP and SP (Table 2) in accordance with previous observations with several phytoplankton species [89]. The effect of nutrient availability on the amount of DCCHO produced and excreted by phytoplankton are often highly species-specific [101].

3.5. Dissolved uronic acids

Initial DUA concentrations of 3.43 ± 0.12 μmol C L^{-1} were determined in the natural seawater used in the *E. huxleyi* cultures. During IP, no-significant differences ($F = 0.13$, $p = 0.891$) were found in the levels of DUA between seawater and seawater enriched with exudates of *E. huxleyi*, in the different pCO_2 treatments, where the average DUA concentration was 3.49 ± 0.10 μmol C L^{-1}. The levels of newly fixed DUA increased for EP and SP. The quantification of DUA in the cultures, corrected to seawater, revealed highest concentrations in treatments with pCO_2 350 μatm (0.56 ± 0.13 μmol C L^{-1} and 2.57 ± 0.16 μmol C L^{-1} for IP and SP respectively) and pCO_2 600 μatm (0.60 ± 0.26 μmol C L^{-1} and 2.69 ± 0.12 μmol C L^{-1} for IP and SP respectively). The concentrations of DUA show a linear correlation with the production of fresh DOC (Figure 4), indicating that the contribution of DUA to

DOC was fairly constant during the experimental cultures. The slope indicates that DUA were responsible for about 1.8% of the DOC released. This value is similar to published values of fractions of DUA to DOC in different marine environments [27,28]. While we did not observe any consistent effect of pCO_2 on the DUA:DOC ratio, the fraction of DUA to DCCHO showed a drastic pH/pCO_2 pattern, increasing during SP from 12.2% to 19.1% when the partial pressure of CO_2 rose from 225 µatm to 900 µatm (Figure 5). Similarly, the computed DUA fractions are in agreement with the values obtained by other authors in different natural systems with high primary production conditions, where the concentrations of DUA accounted for about 0.7 to 5.3% of the DOC and 4.2 to 17.2% of the DCCHO [20,102]. In laboratory studies with continuous cultures of *E. huxleyi*, DUA ranged between 5 and 25% of high molecular weight combined carbohydrates [64].

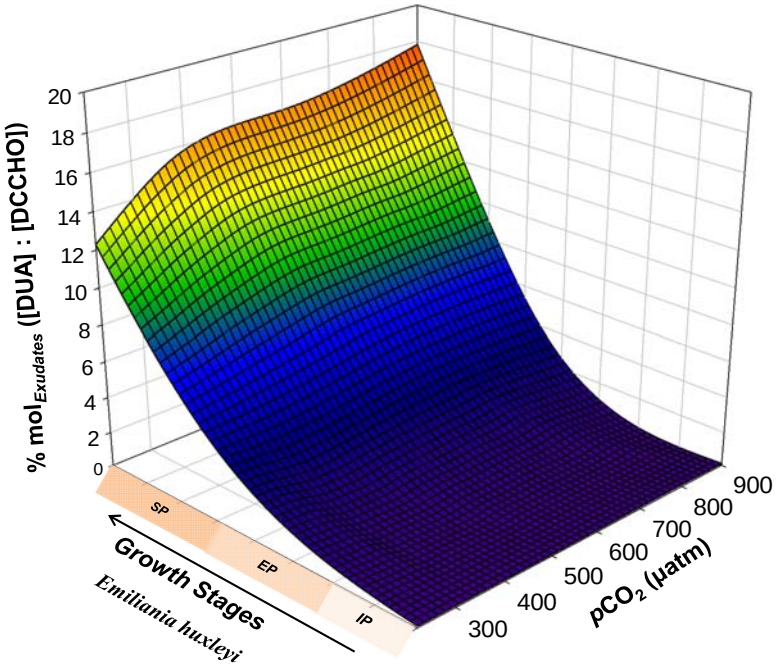

Figure 5. 3D-model contribution of freshly dissolved uronic acids to dissolved carbohydrates released by *E. huxleyi* cultures during the different growth stages (IP: Initial phase; EP: exponential phase and SP: steady phase) under different ocean acidification and major nutrient replete conditions. Tª 25 ºC.

Table 2 shows that DUA_{ER} concurrently increased with the rise in DOC_{ER}. In all CO_2 treatments DUA_{ER} was maximal in the SP. During the period of exponential growth (EP) statistically insignificant differences in DUA_{ER} were observed between treatments (Table 2). However, in SP, DUA_{ER} significantly varied due to changes in the CO_2 conditions and was higher at pCO_2 900 µatm (7.39 ± 0.30 fmol C $cell^{-1}$ day^{-1}) than pCO_2 225 µatm (5.24 ± 0.30 fmol C $cell^{-1}$ day^{-1}; Tukey contrast: t value = 4.206; $p < 0.05$) and pCO_2 350 µatm (6.25 ± 0.48 fmol C $cell^{-1}$ day^{-1}; Tukey contrast: t value = 2.834; $p < 0.1$), whereas at pCO_2 600 (6.70 ± 0.97 fmol C $cell^{-1}$ day^{-1}) it was higher than at pCO_2 225 µatm (Tukey contrast: t value = 2.864; $p < 0.1$) (Table 2). DUA are a major constituent of the carbohydrates found in *E. huxleyi* exudates during exponential and steady growth phases (Figure 5). They have been recognized as a dominant surface-active fraction of extracellular

polymeric substances produced by eukaryotic phytoplankton [103]. Additionally, *in vitro* experiments carried out with seawater from the Southern Ocean have shown that the presence of DUA and uronic acids-rich extracellular polymeric substances enhanced iron bioavailability, yielding an increase in the growth of autochthonous eukaryotic populations [41]. Therefore future alterations of DUA_{ER}, due to ocean acidification, might be a crucial driver of a change in the speciation of iron in marine systems, with consequent implications on its bioavailability [104].

4. Conclusions

The results presented in this study indicated that growth rates of *E. huxleyi* under different pCO_2 conditions depend on the microalgal life cycle. Under acidification conditions, an increase in extracellular release potentially represented a physiological response. Growth stages and variation of pH/pCO_2 conditions in the cultures changed the chemical composition of *E.huxleyi* exudates and the release rates of ligands with high capacity to bind trace metals, such as iron. These findings cannot simply be extrapolated to natural systems, because these results were derived from microcosms, which might introduce experimental artifacts [105] (i.e., bottle effects), nevertheless, they revealed new information on how the extracellular organic release from *E. huxleyi* is influenced by acidification conditions and growth phases. Possible effects of rising oceanic CO_2 concentrations on organic ligand excretion rates will therefore play a major role in metal bioavailability in the future ocean [106]. Accordingly, the CO_2-dependence for PhC_{ER} and DUA_{ER} could also have direct effects in Fe-bioavailability. However, in order to ascertain whether the CO_2-estimulated extracellular release of phenolic compounds and uronic acids increases the Fe-bioavailability, additional Fe-uptake experiments need to be conducted under ocean acidification conditions.

Acknowledgments

This study received support from the EACFe Project (CTM2014-52342-P) of the Ministerio de Economía y Competitividad of Spain. G.S.R. participation was supported by the Grant BES-2011-051448 of the Ministerio de Economía y Competitividad. The authors thank Dr. Javier Aristegui and the IOCAG for the measurements of dissolved organic carbon. Thanks are due to Fundação para a Ciência e a Tecnologia (FCT, Portugal), the European Union, QREN, FEDER, and COMPETE for funding the QOPNA research unit (project PEst-C/QUI/UI0062/2013; FCOMP-01-0124-FEDER-037296).

Conflict of interest

The authors declare there is no conflict of interest.

References

1. Gattuso JP, Magnan A, Bille R, et al.(2015) Contrasting futures for ocean and society from different anthropogenic CO_2 emissions scenarios. *Science* 349: aac4722.
2. Sabine CL, Feely RA, Gruber N, et al. (2004) The oceanic sink for anthropogenic CO_2. *Science* 305: 367-371.

3. IPCC Climate Change. Synthesis Report (2014) Contribution of Working Groups I, II and III to the Fifth Assessment Report of the Intergovernmental Panel on Climate Change. In: R.K. Pachauri and L.A. Meyer, Ed. IPCC, Geneva, Switzerland.
4. Engel A, Händel N, Wohlers J, et al. (2011) Effects of sea surface warming on the production and composition of dissolved organic matter during phytoplankton blooms: Results from a mesocosm study. *J Plankton Res* 33: 357-372.
5. Behrenfeld MJ, O'Malley RT, Siegel DA, et al. (2006) Climate-driven trends in contemporary ocean productivity. *Nature* 444: 752-755.
6. Bosc E, Bricaud A, Antoine D (2004) Seasonal and interannual variability in algal biomass and primary production in the Mediterranean Sea, as derived from 4 years of SeaWiFS observations. *Global Biogeochem Cycles* 18: 1-17.
7. Hansell DA (2013) Recalcitrant dissolved organic carbon fractions. *Ann Rev Mar Sci* 5: 421-445.
8. Honjo S, Eglinton T, Taylor C, et al. (2014) Understanding the role of the biological pump in the global carbon cycle. An imperative for Ocean Science. *Oceanogr* 27: 10-16.
9. Carlson CA, Hansell DA (2015) DOM: Sources, sinks, reactivity, and budgets. In: Hansell, D.A., Carlson C.A. *Biogeochemistry of Marine Dissolved Organic Matter*, 2 Eds., Boston Academic Press, 65-126.
10. Agustí S, Duarte CM (2013) Phytoplankton lysis predicts dissolved organic carbon release in marine plankton communities. *Biogeosciences* 10: 1259-1264.
11. Ruiz-Halpern S, Duarte CM, Tovar-Sanchez A, et al. (2011) *Antarctic krill* as a source of dissolved organic carbon to the Antarctic ecosystem. *Limnol Oceanogr* 56: 521-528.
12. Wu Y, Gao K, Riebesell U (2010) CO_2-induced seawater acidification affects physiological performance of the marine diatom *Phaeodactylum tricornutum*. *Biogeosciences* 7: 2915-2923.
13. Engel A, Zondervan I, Aerts K, et al. (2005) Testing the direct effect of CO_2 concentration on a bloom of the coccolithophorid *Emiliania huxleyi* in mesocosm experiments. *Limnol Oceanogr* 50: 493-507.
14. Repeta DJ (2015) Chemical characterization and cycling of Dissolved Organic Matter. In: Hansell, D.A., Carlson C.A. *Biogeochemistry of Marine Dissolved Organic Matter*, 2 Eds., Boston Academic Press, 21-63.
15. Benner R, Pakulski JD, McCarthy M, et al. (1992) Bulk chemical characteristics of dissolved organic matter in the Ocean. *Science* 255: 1561-1564.
16. Leenheer JA, Croué JP (2003) Characterizing aquatic dissolved organic matter. *Environ Sci Technol* 37: 18-26.
17. Benner R (2011) Loose ligands and available iron in the ocean. *Proc Natl Acad Sci USA* 108: 893-894.
18. Kaiser K, Benner R (2009) Biochemical composition and size distribution of organic matter at the Pacific and Atlantic time-series stations. *Mar Chem* 113: 63-77.
19. Hung CC, Guo L, Santschi PH, et al. (2003) Distributions of carbohydrate species in the Gulf of Mexico. *Mar Chem* 81: 119-135.
20. Hung CC, Tang D, Warnken KW, et al. (2001) Distributions of carbohydrates, including uronic acids, in estuarine waters of Galveston Bay. *Mar Chem* 73: 305-318.
21. Bourgoin LH, Tremblay L (2010) Bacterial reworking of terrigenous and marine organic matter in estuarine water columns and sediments. *Geochim Cosmochim Acta* 74: 5593-5609.

22. Jørgensen L, Lechtenfeld OJ, Benner R, et al. (2014) Production and transformation of dissolved neutral sugars and amino acids by bacteria in seawater. *Biogeosciences* 11: 5349-5363.
23. Piontek J, Borchard C, Sperling M, et al. (2013) Response of bacterioplankton activity in an Arctic fjord system to elevated pCO_2: Results from a mesocosm perturbation study. *Biogeosciences* 10: 297-314.
24. Galgani L, Piontek J, Engel A (2016) Biopolymers form a gelatinous microlayer at the air-sea interface when Arctic sea ice melts. *Sci Rep* 6: 29465.
25. Underwood GJC, Aslam SN, Michel C, et al. (2013) Broad-scale predictability of carbohydrates and exopolymers in Antarctic and Arctic sea ice. *Proc Natl Acad Sci USA* 110: 15734-15739.
26. Hassler CS, Alasonati E, Mancuso-Nichols CA, et al. (2011) Exopolysaccharides produced by bacteria isolated from the pelagic Southern Ocean - Role in Fe binding, chemical reactivity, and bioavailability. *Mar Chem* 123: 88-98.
27. Verdugo P, Alldredge AL, Azam F, et al. (2004) The oceanic gel phase: A bridge in the DOM-POM continuum. *Mar Chem* 92: 67-85.
28. Engel A, Thoms S, Riebesell U, et al. (2004) Polysaccharide aggregation as a potential sink of marine dissolved organic carbon. *Nature* 428: 929-932.
29. Stubbins A, Hubbard V, Uher G, et al. (2008) Relating carbon monoxide photoproduction to dissolved organic matter functionality. *Environ Sci Technol* 42: 3271-3276.
30. Li F, Pan B, Zhang D, et al. (2015) Organic matter source and degradation as revealed by molecular biomarkers in agricultural soils of Yuanyang terrace. *Sci Rep* 5: 11074.
31. Lu CJ, Benner R, Fichot CG, et al. (2016) Sources and transformations of dissolved lignin phenols and chromophoric dissolved organic matter in Otsuchi Bay, Japan. *Front Mar Sci* 3: 1-12.
32. Klappe L, McKnight DM, Fulton JR, et al. (2002) Fulvic acid oxidation state detection using fluorescence spectroscopy. *Environ Sci Technol* 36: 3170-3175.
33. Helms JR, Mao J, Chen H, et al. (2015). Spectroscopic characterization of oceanic dissolved organic matter isolated by reverse osmosis coupled with electrodialysis. *Mar Chem* 177: 278-287.
34. López-Alarcón C, Denicola A (2013) Evaluating the antioxidant capacity of natural products: A review on chemical and cellular-based assays. *Anal Chim Acta* 763: 1-10.
35. Rico M, Santana-Casiano JM, González AG, et al. (2013) Variability of the phenolic profile in the diatom *Phaeodactylum tricornutum* growing under copper and iron stress. *Limnol Oceanogra* 51: 144-152.
36. López A, Rico M, Santana-Casiano JM, et al. (2015) Phenolic profile of *Dunaliella tertiolecta* growing under high levels of copper and iron. *Environ Sci Pollut Res* 22: 14820-14828.
37. Elhabiri M, Carrër C, Marmolle F, et al. (2007) Complexation of iron(III) by catecholate-type polyphenols. *Inorg Chim Acta* 360: 353-359.
38. Sreeram KJ, Shrivastava HY, Nair BU (2004) Studies on the nature of interaction of iron(III) with alginates. *Biochim Biophys Acta* 1670: 121-125.
39. Santana-Casiano JM, González-Dávila M, González AG, et al. (2014) Characterization of phenolic exudates from *Phaeodactylum tricornutum* and their effects on the chemistry of Fe(II)-Fe(III). *Mar Chem* 158: 10-16.
40. Wu Y, Xiang W, Fu X, et al. (2016) Geochemical interactions between iron and phenolics originated from peatland in Hani, China: implications for effective transport of iron from terrestrial systems to marine. *Environ Earth Sci* 75: 336.

41. Hassler CS, Schoemann V (2009) Bioavailability of organically bound Fe to model phytoplankton of the Southern Ocean. *Biogeosciences* 6: 2281-2296.
42. Maldonado MT, Strzepek RF, Sander S, et al. (2005) Acquisition of iron bound to strong organic complexes, with different Fe binding groups and photochemical reactivities, by plankton communities in Fe-limited subantarctic waters. *Global Biogeochem Cycles* 19: Gb4S23.
43. Hassler CS, Schoemann V, Nichols CM, et al. (2011) Saccharides enhance iron bioavailability to Southern Ocean phytoplankton. *Proc Natl Acad Sci USA* 108: 1076-1081.
44. Gordon RM, Martin JH, Knauer GA (1982) Iron in north-east Pacific waters. *Nature* 299: 611-612.
45. Heller MI, Wuttig K, Croot PL (2016) Identifying the Sources and Sinks of CDOM/FDOM across the Mauritanian Shelf and their potential role in the decomposition of superoxide (O_2^-). *Front Mar Sci* 3: 132.
46. Hassler CS, Norman L, Mancuso-Nichols CA, et al. (2015) Iron associated with exopolymeric substances is highly bioavailable to oceanic phytoplankton. *Mar Chem* 173: 136-147.
47. Mueller B, den Haan J, Visser PM, et al. (2016) Effect of light and nutrient availability on the release of dissolved organic carbon (DOC) by Caribbean turf algae. *Sci Rep* 6: 23248.
48. Gunderson AR, Armstrong EJ, Stillman JH (2016) Multiple stressors in a changing world: The need for an improved perspective on physiological responses to the dynamic marine environment. *Annu Rev Mar Sci* 8: 357-378.
49. Jin P, Wang T, Liu N, et al. (2015) Ocean acidification increases the accumulation of toxic phenolic compounds across trophic levels. *Nat Commun 6*: 8714.
50. Lidbury I, Johnson V, Hall-Spencer JM, et al. (2012) Community-level response of coastal microbial biofilms to ocean acidification in a natural carbon dioxide vent ecosystem. *Mar Pollut Bull* 64: 1063-1066.
51. Borchard C, Engel A (2012) Organic matter exudation by *Emiliania huxleyi* under simulated future ocean conditions. *Biogeosciences* 9: 3405-3423.
52. Barofsky A, Vidoudez C, Pohnert G (2009) Metabolic profiling reveals growth stage variability in diatom exudates. *Limnol Oceanogr Methods* 7: 382-390.
53. Doney SC, Fabry VJ, Feely RA, et al. (2009) Ocean Acidification: The other CO_2 problem. *Annu Rev Mar Sci 1*: 169-192.
54. Read BA, Kegel J, Klute MJ (2013) Pan genome of the phytoplankton *Emiliania* underpins its global distribution. *Nature* 499: 209-213.
55. Riebesell U, Fabry VJ, Hansson L, et al. (2010) Guide to best practices in Ocean Acidification research and data reporting. *European Commisson,* ISBN 9789279111181.
56. Achterberg EP, Holland TW, Bowie AR, et al. (2001) Determination of iron in seawater. *Anal Chim Acta*, 442: 1-14.
57. González-Dávila M, Santana-Casiano JM, Rueda MJ, et al. (2010) The water column distribution of carbonate system variables at the ESTOC site from 1995 to 2004. *Biogeosciences* 7: 3067-3081.
58. Millero FJ, Graham TB, Huang F, et al. (2006) Dissociation constants of carbonic acid in seawater as a function of salinity and temperature. *Mar Chem* 100: 80-94.
59. Arístegui J, Duarte CM, Reche I, et al. (2014) Krill excretion boosts microbial activity in the Southern Ocean. *PLoS ONE* 9: e89391.
60. Arnow LE (1937) Colorimetric determination of the components of

3,4-dihydroxyphenylalaninetyrosine mixtures. *J Biol Chem* 118: 531-537.
61. Myklestad SM, Skänoy E, Hestmann S (1997). A sensitive and rapid method for analysis of dissolved mono- and polysaccharides in nseawater. *Mar Chem* 56: 279-286.
62. Blumenkrantz N, Asboe-Hansen G (1973) New method for quantitative determination of uronic acids. *Anal Biochem* 54: 484-489.
63. Bastos R, Coelho E, Coimbra MA (2015) Modifications of *Saccharomyces pastorianus* cell wall polysaccharides with brewing process. *Carbohydr Polym* 124: 322-330.
64. Borchard C, Engel A (2015) Size-fractionated dissolved primary production and carbohydrate composition of the coccolithophore *Emiliania huxleyi*. *Biogeosciences* 12: 1271-1284.
65. Müller MN, Antia A, La Roche J (2008) Influence of cell cycle phase on calcification in the coccolithophore *Emiliania huxleyi*. *Limnol Oceanogr* 53: 506-512.
66. Daniels CJ, Sheward RM, Poulton AJ (2014) Biogeochemical implications of comparative growth rates of *Emiliania huxleyi* and Coccolithus species. *Biogeosciences* 11: 6915-6925.
67. Müller MN, Schulz KG, Riebesell U (2010) Effects of long-term high CO_2 exposure on two species of coccolithophores. *Biogeosciences* 6: 10963-10982.
68. Langer G, Nehrke G, Probert I, et al. (2009). Strain-specific responses of *Emiliania huxleyi* to changing seawater carbonate chemistry. *Biogeosciences* 6: 4361-4383.
69. Bach LT, Bauke C, Meier KJS, et al. (2012) Influence of changing carbonate chemistry on morphology and weight of coccoliths formed by E*miliania huxleyi*. *Biogeosciences* 9: 3449-3463.
70. Meyer J, Riebesell U (2015) Reviews and syntheses: Responses of coccolithophores to ocean acidification: A meta-analysis. *Biogeosciences* 12: 1671-1682.
71. Rokitta SD, Rost B (2012) Effects of CO_2 and their modulation by light in the life-cycle stages of the coccolithophore *Emiliania huxleyi*. *Limnol Oceanogr* 57: 607-618.
72. Sett S, Bach LT, Schulz KG, et al. (2014) Temperature modulates coccolithophorid sensitivity of growth, photosynthesis and calcification to increasing seawater pCO_2. *PLoS ONE* 9: e0088308.
73. Sciandra A, Harlay J, Lefèvre D, et al. (2003) Response of coccolithophorid *Emiliania huxleyi* to elevated partial pressure of CO_2 under nitrogen limitation. *Mar Ecol Prog Ser* 261: 111-122.
74. Riegman R, Stolte W, Noordeloos AAM, et al. (2000) Nutrient uptake and alkaline phosphatase activity of *Emiliania huxleyi* (Prymnesiophyceae) during growth under N and P limitation in continuous cultures. *J Phycol* 36: 87-96.
75. Zondervan I (2007) The effects of light, macronutrients, trace metals and CO_2 on the production of calcium carbonate and organic carbon in coccolithophoridores-A review. *Deep-Sea Res Part II: Top Stud Oceanogr* 54: 521-537.
76. Nielsdóttir MC, Moore CM, Sanders R, et al. (2009) Iron limitation of the postbloom phytoplankton communities in the Iceland Basin. *Global Biogeochem Cycles* 23: 1-13.
77. Tagliabue A, Mtshali T, Aumont O, et al. (2012) A global compilation of dissolved iron measurements: Focus on distributions and processes in the Southern Ocean. *Biogeosciences* 9: 2333-2349.
78. Sherr EB, Sherr BF, Wheeler PA (2005) Distribution of coccoid cyanobacteria and small eukaryotic phytoplankton in the upwelling ecosystem off the Oregon coast during 2001 and 2002. *Deep-Sea Res Part II: Top Stud Oceanogr* 52: 317-330.
79. Alexov EG, Gunner MR (1997) Incorporating protein conformational flexibility into the calculation of pH-dependent protein properties. *Biophys J* 72: 2075-2093.
80. Riebesell U, Schulz KG, Bellerby RGJ, et al. (2007) Enhanced biological carbon consumption

in a high CO_2 ocean. *Nature* 450: 545-548.
81. MacGilchrist GA, Shi T, Tyrrell T, et al. (2014) Effect of enhanced pCO_2 levels on the production of dissolved organic carbon and transparent exopolymer particles in short-term bioassay experiments. *Biogeosciences* 11: 3695-3706.
82. Paul AJ, Bach LT, Schulz KG, et al. (2015) Effect of elevated CO_2 on organic matter pools and fluxes in a summer Baltic Sea plankton community. *Biogeosciences* 12: 6181-6203,.
83. Yoshimura T, Suzuki K, Kiyosawa H, et al. (2013) Impacts of elevated CO_2 on particulate and dissolved organic matter production: Microcosm experiments using iron-deficient plankton communities in open subarctic waters. *J Oceanogr* 69: 601-618.
84. Thornton DCO (2014) Dissolved organic matter (DOM) release by phytoplankton in the contemporary and future ocean . *Eur J Phycol* 49: 20-46.
85. Spilling K, Schulz KG, Paul AJ, et al. (2016) Effects of ocean acidification on pelagic carbon fluxes in a mesocosm experiment. *Biogeosciences* 13: 6081-6093.
86. Becker JW, Berube PM, Follett CL, et al. (2014) Closely related phytoplankton species produce similar suites of dissolved organic matter. *Front Microbio* 5: 1-14.
87. Underwood GJC, Boulcott M, Raines CA, et al. (2004) Environmental effects on exopolymeric production by marine benthic diatoms: Dynamics, changes in composition and pathways of production. *J Phycol* 40: 293-304.
88. Wetz MS, Wheeler PA (2007). Release of dissolved organic matter by coastal diatoms. *Limnol Oceanogr* 52: 798-807.
89. Van Oostende N, Moerdijk-Poortvliet TCW, Boschker HTS, et al. (2013) Release of dissolved carbohydrates by *Emiliania huxleyi* and formation of transparent exopolymer particles depend on algal life cycle and bacterial activity. *Environ Microbio* 15: 1514-1531.
90. Biddanda B, Benner R (1997) Carbon, nitrogen, and carbohydrate fluxes during the production of particulate and dissolved organic matter by marine phytoplankton. *Limnol Oceanogr* 42: 506-518.
91. Engel A, Piontek J, Grossart HP, et al. (2014) Impact of CO_2 enrichment on organic matter dynamics during nutrient induced coastal phytoplankton blooms. *J Plankton Res* 36: 641-657.
92. Song C, Ballantyne IVF, Smith VH (2014) Enhanced dissolved organic carbon production in aquatic ecosystems in response to elevated atmospheric CO_2. *Biogeochem* 118: 49-60.
93. Zubia M, Payri C, Deslandes E (2016) Alginate, mannitol, phenolic compounds and biological activities of two range-extending brown algae, *Sargassum mangarevense* and *Turbinaria ornata* (*Phaeophyta: Fucales*), from Tahiti (French Polynesia). *J Appl Phycol* 20: 1033-1043.
94. Celis-Plá PSM, Bouzon ZL, Hall-Spencer JM, et al. (2016) Seasonal biochemical and photophysiological responses in the intertidal macroalga *Cystoseira tamariscifolia (Ochrophyta)*. *Mar Environ Res* 115: 89-97.
95. Huang JJH, Xu WW, Lin SL, et al. (2016) Phytochemical profiles of marine phytoplanktons: an evaluation of their in vitro antioxidant and anti-proliferative activities. *Food Funct* 7: 5002-5017.
96. Celis-Plá PSM, Hall-Spencer JM, Horta PA, et al. (2015) Macroalgal responses to ocean acidification depend on nutrient and light levels. *Front Mar Sci* 2: 1-12.
97. Shi D, Xu Y, Hopkinson BM, et al. (2010) Effect of ocean acidification on iron availability to marine phytoplankton. *Science* 327: 676-679.
98. Gledhill M, McCormack P, Ussher S, et al. (2004) Production of siderophore type chelates by mixed bacterioplankton populations in nutrient enriched seawater incubations. *Mar Chem* 88: 75-83.
99. Kranzler C, Lis H, Finkel OM, et al. (2014) Coordinated transporter activity shapes high-affinity

iron acquisition in cyanobacteria. *ISME J* 8: 409-417.
100. Manwar AV, Khandelwal SR, Chaudhari BL, et al. (2004) Siderophore production by a marine *Pseudomonas aeruginosa* and its antagonistic action against phytopathogenic fungi. *Appl Biochem Biotechnol* 118: 243-251.
101. Urbani R, Magaletti E, Sist P, et al. (2005) Extracellular carbohydrates released by the marine diatoms *Cylindrotheca closterium, Thalassiosira pseudonana* and *Skeletonema costatum*: Effect of P-depletion and growth status. *Sci Total Environ* 353: 300-306.
102. Khodse VB, Bhosle NB, Matondkar SGP (2010) Distribution of dissolved carbohydrates and uronic acids in a tropical estuary, India. *J Earth Syst Sci* 119: 519-530.
103. Ozturk S, Aslim B, Suludere Z, et al. (2014) Metal removal of cyanobacterial exopolysaccharides by uronic acid content and monosaccharide composition. *Carbohydr Polym* 101: 265-271.
104. Hutchins DA, Boyd PW (2016) Marine phytoplankton and the changing ocean iron cycle. *Nat Clim Change* 6: 1072-1079,
105. Geider RJ, La Roche J (1994) The role of iron in phytoplankton photosynthesis, and the potential for iron-limitation of primary productivity in the sea. *Photosynth Res* 39: 275-301.
106. Hoffmann LJ, Breitbarth E, Boyd PW, et al. (2012) Influence of ocean warming and acidification on trace metal biogeochemistry. *Mar Ecol Prog Ser* 470: 191-205.

AIMS Press